Use of Damaged DNA and dNTP Substrates by the Error-Prone DNA Polymerase X from African Swine Fever Virus†

Sandeep Kumar,‡ Brandon J. Lamarche,‡ and Ming-Daw Tsai*

Departments of Chemistry and Biochemistry, The Biophysics Program, and The Ohio State Biochemistry Program, The Ohio State University, Columbus, Ohio 43210, and Genomics Research Center, Academia Sinica, Taiwan

Received July 25, 2006; Revised Manuscript Received December 22, 2006

ABSTRACT: The structural specificity that translesion DNA polymerases often show for a particular class of lesions suggests that the predominant criterion of selection during their evolution has been the capacity for lesion tolerance and that the error-proneness they display when copying undamaged templates may simply be a byproduct of this adaptation. Regardless of selection criteria/evolutionary history, at present both of these properties coexist in these enzymes, and both properties confer a fitness advantage. The repair polymerase, Pol X, encoded by the African swine fever virus (ASFV) is one of the most error-prone polymerases known, leading us to previously hypothesize that it may work in tandem with the exceptionally error-tolerant ASFV DNA ligase to effect viral mutagenesis. Here, for the first time, we test whether the error-proneness of Pol X is coupled with a capacity for lesion tolerance by examining its ability to utilize the types of damaged DNA and dNTP substrates that are expected to be relevant to ASFV. We (i) test Pol X's ability to both incorporate opposite to and extend from ubiquitous oxidative purine (7,8-dihydro-8-oxoguanine), oxidative pyrimidine (5,6-dihydroxy-5,6-dihydrothymine), and non-coding (AP site) lesions, in addition to 5,6-dihydrothymine, (ii) determine the catalytic efficiency and dNTP specificity of Pol X when catalyzing incorporation opposite to, and when extending from, 7,8-dihydro-8-oxoguanine in a template/primer context, and (iii) quantitate Pol X-catalyzed incorporation of the damaged nucleotide 8-oxo-dGTP opposite to undamaged templates in the context of both template/primer and a single-nucleotide gap. Our findings are discussed in light of ASFV biology and the mutagenic DNA repair hypothesis described above.

First identified in Kenya in the early 1900s when imported domestic swine contracted a disease of high lethality, ASFV[1] has subsequently been detected in forms of varying virulence/lethality throughout Africa, the Iberian Peninsula, the Caribbean, and South America (*1*). Since neither a vaccine to prevent ASFV infection nor a treatment for infected pigs is currently available, ASFV outbreaks are controlled by slaughter of infected and exposed animals, making the disease economically important. ASFV is now known to be a large [168−189 kb (*2*)] double-stranded DNA virus that encodes 151 proteins (*3*) and displays a tropism for macrophages and monocytes (*4*). Though it utilizes the host cell nucleus during an early phase of viral DNA synthesis, subsequent replication/assembly of the ASFV genome occurs in cytoplasmic/perinuclear viral factories (*5*−*7*), and consistent with this, the virus encodes its own replicative DNA polymerase in addition to a simple DNA repair system consisting of an AP endonuclease (APE), a repair polymerase (Pol X), and an ATP-dependent DNA ligase[2] (*3*).

Having demonstrated that Pol X is extremely error-prone during single-nucleotide gap filling (*9*, *10*) and that the downstream ASFV DNA ligase is the most error-tolerant DNA ligase known (*11*), we have hypothesized that the ASFV DNA repair system may be mutagenic (*8*, *9*, *11*, *12*). By replacing damaged nucleotides with undamaged but incorrect nucleotides, the sequential action of Pol X and ASFV DNA ligase could introduce point mutations into the viral genome, thereby contributing to the genetic (*13*) and antigenic (*14*) diversity known to exist among different ASFV isolates. Alternative rationales for the unusual substrate specificities of Pol X and ASFV DNA ligase can, however, be envisioned and ought to be evaluated. The work described here was undertaken as part of an ongoing effort to elucidate a molecular and biological rationale for the extreme error-proneness of Pol X. Being unable to perform

† This work was supported by NIH Grant GM43268. B.J.L. was supported in part by a predoctoral NIH CBIP fellowship (2T32 GM08512).

* To whom correspondence should be addressed at the Department of Chemistry [phone, (614) 292-3080; fax, (614) 292-1532; e-mail, tsai@chemistry.ohio-state.edu].

‡ Department of Chemistry only.

[1] Abbreviations: AP, apurinic/apyrimidinic; APE, AP endonuclease; ASFV, African swine fever virus; BSA, bovine serum albumin; deazaA, 7-deazaadenine; 7-deaza-dATP, 7-deaza-2′-deoxyadenosine 5′-triphosphate; DHT, 5,6-dihydrothymine; DTT, dithiothreitol; f_{inc}, misincorporation ratio; 8-oxo-G, 7,8-dihydro-8-oxoguanine; 8-oxo-dGTP, 7,8-dihydro-8-oxo-2′-deoxyguanosine 5′-triphosphate; PNK, polynucleotide kinase; Pol, DNA polymerase; ROS, reactive oxygen species; Tg, 5,6-dihydroxy-5,6-dihydrothymine (thymine glycol); THF, tetrahydrofuran; TLS, translesion synthesis.

[2] Note that a DNA glycosylase is conspicuously absent from this DNA repair system. This has led us and others to hypothesize that these genes have been retained in the viral genome for the purpose of processing spontaneously generated AP sites and/or reactive oxygen species- (ROS-) induced single-strand breaks (*8*).

10.1021/bi061501l CCC: $37.00
Published on Web 03/03/2007

Table 1: The Most Error-Prone DNA Polymerases Known Also Display Translesion Synthesis Capabilities

enzyme	fidelity when copying undamaged templates (range of f_{inc})[a]	translesion synthesis activity[c]
mammalian Pol ι	$6.7 \times 10^{-1}-1.0 \times 10^{-4}$ (*66*)	bypass of alkylated bases (*67*) bypass of thymine *cis*−*syn* dimers (*20*, *68*) bypass of pyrimidine (6-4) pyrimidone photoproduct (*68*)
ASFV Pol X	**$3.5 \times 10^{-1}-1.3 \times 10^{-4}$ (*9*, *10*)[b]**	**this study**
mammalian Pol κ	$5.8 \times 10^{-2}-5.2 \times 10^{-4}$ (*69*)	bypass of AP sites (*70*) bypass of bulky adducts (*71*, *72*) bypass of oxidative damage (*34*) bypass of nitration-damaged bases (*73*) extension from lesion-containing base pairs (*22*, *74*, *75*) extension from mismatched primer termini (*76*)
mammalian Pol η	$1.1 \times 10^{-2}-1.1 \times 10^{-3}$ (*77*)	bypass of thymine *cis*−*syn* dimers (*78*) bypass of pyrimidine (6-4) pyrimidone photoproduct (*79*) bypass of *cis*-platin-induced damage (*80*) bypass of AP sites (*81*) bypass of bulky adducts (*82*, *83*) bypass of alkylated bases (*67*, *84*) bypass of oxidative damage (*35*, *85*) bypass of nitration-damaged bases (*73*)
E. coli Pol V	$4.8 \times 10^{-3}-<1.0 \times 10^{-5}$ (*86*)	bypass of AP sites (*86*, *87*) bypass of thymine *cis*−*syn* dimers (*86*) bypass of pyrimidine (6-4) pyrimidone photoproduct (*86*) bypass of bulky adducts (*88*, *89*)
S. solfataricus Dpo4	$3.2 \times 10^{-3}-1.5 \times 10^{-4}$ (*90*)	bypass of AP sites (*81*) bypass of thymine *cis*−*syn* dimers (*91*) bypass of oxidative damage (*45*) bypass of bulky adducts (*92*, *93*)
E. coli Pol IV	$1.7 \times 10^{-3}-3.6 \times 10^{-5}$ (*86*)	bypass of AP sites (*94*) bypass of bulky adducts (*71*, *72*, *88*) extension from misaligned primer termini (*95*)

[a] Fidelity (i.e., error-proneness) is quantitatively represented here using the misincorporation ratio (f_{inc}). For data obtained in the steady state (Pols ι, κ, η, V, and IV), $f_{inc} = (V_{max}/K_M)_{incorrect}/(V_{max}/K_M)_{correct}$. For data obtained in the pre-steady state (Pol X and Dpo4), $f_{inc} = (k_{pol}/K_{d,app})_{incorrect}/(k_{pol}/K_{d,app})_{correct}$. Range of f_{inc} indicates the misincorporation ratio for the lowest and highest fidelity base pair for each enzyme. While fidelity data for Pol X were obtained using a single-nucleotide gapped substrate, fidelity data for all other polymerases were obtained using template/primer substrates. [b] The f_{inc} values for Pol X are derived both from ref *9* (all mismatched base pairs other than G·G) and from ref *10* (the G·G base pair). [c] Rather than using specific lesion names, lesions are typically listed by general category. This list is not meant to be exhaustive.

experiments with intact ASFV,[3] herein we employ in vitro assays to test whether the relaxed substrate specificity of Pol X might serve a purpose other than, or in addition to, the posited mutagenesis described above.

Recently, a large number of novel DNA polymerases from all three kingdoms of life have been shown to replicate DNA with very low fidelity (*15*, *16*). Consistent with this property, when these enzymes are permitted access to DNA, they are capable of conferring a fitness advantage by generating genetic diversity (*15*, *17*, *18*). However, error-proneness may not have been the predominant criterion of selection during the evolution of these polymerases: the ability to incorporate nucleotides opposite to (*19*−*21*) or immediately downstream of (*22*, *23*) DNA lesions that would otherwise hinder the replisome suggests that many of these enzymes have primarily been selected for translesion synthesis (TLS) capabilities and that error-proneness when copying *undamaged* templates may simply be a byproduct, albeit a potentially useful one, of this adaptation. In support of this interpretation is the fact that TLS polymerases often display active site-DNA-dNTP interaction networks which are not merely spacious/nonrestrictive but, rather, which are specifically tailored for utilization of a particular lesion or class of lesions (*24*−*27*). However, regardless of which property (TLS vs error-proneness on undamaged templates) was the primary criterion of evolutionary selection, at the present time both properties coexist in TLS polymerases (Table 1), and current data suggest that both properties are in fact utilized to achieve a fitness advantage (*15*, *16*). Does Pol X also serve these dual purposes in ASFV? Is the known error-proneness of Pol X coupled with a capacity for lesion tolerance? While identification of TLS activity in Pol X would not discount a role in mutagenic DNA repair, it would provide an alternative explanation for how/why this viral polymerase came to be so error-prone. Alternatively, the absence of TLS activity in Pol X would suggest that error-proneness (or perhaps some other as of yet undefined catalytic property) was the dominant selective pressure in its evolution.

By examining the ability of Pol X to utilize the types of damaged DNA and dNTP substrates that are expected to be relevant to ASFV, herein we explore whether the low fidelity of this polymerase is coupled with a capacity for lesion tolerance. Toward this end, we first qualitatively test Pol X's ability to both incorporate opposite to and extend from the common oxidative lesions 7,8-dihydro-8-oxoguanine (8-oxo-G) and 5,6-dihydroxy-5,6-dihydrothymine (Tg), in addition to 5,6-dihydrothymine (DHT) and a noncoding lesion (AP site). We then determine the catalytic efficiency and dNTP specificity of Pol X when catalyzing incorporation opposite to 8-oxo-G, as well as extension from the resultant 8-oxo-G-containing base pair, in a template/primer context. The

[3] The U.S. Department of Agriculture has classified ASFV as a "select agent", and the BSL3+ facilities required for working with the virus are not currently available to us.

Table 2: DNA Substrates

assay to be used in	sequence[a]	description
translesion synthesis	5′-^{32}P-GCCTCGCAGCCGTCCAACC 3′-CGGAGCGTCGGCAGGTTGGTTGAGT**X**CGAGCTAGGTTACGGCAGG	**X** = 8-oxo-G, Tg, or an AP site
translesion synthesis	5′-^{32}P-GGACGGCATTGGATC 3′-CCTGCCGTAACCTAGCTCC**X**ACTCAACCAACCTGCCGACGCTCCG	**X** = DHT
extension from AP site- and Tg-containing base pairs	5′-^{32}P-GCCTCGCAGCCGTCCAACCAACTCA**Z** 3′-CGGAGCGTCGGCAGGTTGGTTGAGT**X**CGAGCTAGGTTACGGCAGG	**X** = an AP site or Tg; **Z** = A, T, G, or C
extension from 8-oxo-G-containing base pairs	5′-^{32}P-GCCTCGCAGCCGTCCAACCAACTCA**Z** 3′-CGGAGCGTCGGCAGGTTGGTTGAGT**X**CGAGCTAGGTTACGGCAGG	**X** = 8-oxo-G or G (control); **Z** = A or C
incorporation of dATP, 7-deaza-dATP, dTTP, or dCTP opposite to 8-oxo-G	5′-^{32}P-GCCTCGCAGCCGTCCAACCAACTCA 3′-CGGAGCGTCGGCAGGTTGGTTGAGT**X**CGAGCTAGGTTACGGCAGG	**X** = 8-oxo-G or G (control)
incorporation of dGTP opposite to 8-oxo-G	5′-^{32}P-GCCTCGCAGCCGTCCAACCAACTCA 3′-CGGAGCGTCGGCAGGTTGGTTGAGT**X**TGAGCTAGGTTACGGCAGG	**X** = 8-oxo-G
incorporation of 8-oxo-dGTP	5′-^{32}P-GCCTCGCAGCCGTCCAACCAACTCA 3′-CGGAGCGTCGGCAGGTTGGTTGAGT**X**CGAGCTAGGTTACGGCAGG	**X** = A or C
incorporation of 8-oxo-dGTP or dGTP (control)	5′-^{32}P-GCCTCGCAGCCGTCCAACCAACTCA GCTCGATCCAATGCCGTCC 3′-CGGAGCGTCGGCAGGTTGGTTGAGT**X**CGAGCTAGGTTACGGCAGG	**X** = A or C

[a] In the single-nucleotide gapped substrate the downstream oligonucleotide is 5′-phosphorylated.

glycosidic conformation (*anti* vs *syn*) of incoming dATP in the 8-oxo-G·A base pair is then probed using the nucleotide analogue 7-deaza-2′-deoxyadenosine 5′-triphosphate (7-deaza-dATP). Finally, we quantitate Pol X-catalyzed incorporation of the damaged nucleotide 8-oxo-dGTP opposite to undamaged templates in the context of a template/primer as well as a single-nucleotide gap. The implications of these findings on ASFV fitness and adaptability are discussed.

EXPERIMENTAL PROCEDURES

Materials. Bovine serum albumin (BSA) was from Roche. Standard oligonucleotides, in addition to the one containing the tetrahydrofuran (THF) abasic site analogue (which lacks the C1′ hydroxyl of ribose and therefore is not prone to β-elimination), were from Integrated DNA Technologies (IDT). Oligonucleotides containing the lesions 8-oxo-G, Tg, and DHT were from Synthegen (now IDT). 8-Oxo-dGTP and 7-deaza-dATP were from TriLink BioTechnologies. [γ-^{32}P]ATP and Microspin G-25 columns were from Amersham Biosciences. T4 polynucleotide kinase (PNK) was from New England Biolabs. Sep-Pak C18 columns were from Waters. Materials and reagents not listed here were of standard molecular biology grade.

Protein Expression, Purification, and Quantitation. Pol X was expressed and purified as described (*9*) except that the protein was supplemented with glycerol to a final concentration of 40% (v/v) prior to storage at −80 °C. The concentration of active protein was determined by burst assays using a KinTek RQF-3 rapid chemical quench apparatus as described previously (*10*).

Preparation of DNA Substrates. Oligonucleotides were purified by polyacrylamide gel electrophoresis and were then extracted into a buffer consisting of 500 mM ammonium acetate and 1 mM EDTA (pH 7.5), desalted on Sep-Pak C18 columns, dried in a CentriVap, and finally resuspended in TE buffer (10 mM Tris-HCl, 1 mM EDTA, pH 7.5) prior to storage at −20 °C. The concentration of purified oligonucleotides was determined by UV absorbance at 260 nm using extinction coefficients provided by the respective vendors. Upstream primers were ^{32}P labeled at their 5′ termini using [γ-^{32}P]ATP and PNK. After heat inactivating PNK at 65 °C for 20 min, free [γ-^{32}P]ATP was removed on Microspin G-25 columns. All DNA substrates (Table 2) were assembled at room temperature by mixing primer/template/downstream oligo (when applicable) in a 1:1.1:1.2 molar ratio. Typically, only 5% of the substrate molecules were ^{32}P labeled. Once assembled, substrates were diluted into "assay buffer" [50 mM Tris−borate, 140 mM KCl, 3% glycerol, pH 7.5 (adjusted at 37 °C)] and stored at 4 °C prior to use.

Steady State Translesion Synthesis Assays. The ability of Pol X to incorporate nucleotides upstream of, opposite to, and downstream of a templating lesion was examined qualitatively using steady state running-start assays. The template/primer substrates allowed Pol X to incorporate either four or six nucleotides before encountering the templating lesion (see Table 2 for substrate details). Polymerase reactions were conducted at 37 °C in the above assay buffer by manually mixing a protein solution (100 nM Pol X, 200 μg/mL BSA, 2 mM DTT, 1 mM each of the four dNTPs, and 20 mM *free*[4] $MgCl_2$) with a DNA solution (200 nM template/primer) in a 1:1 ratio. Aliquots (10 μL) of the reaction were subsequently quenched by mixing with 10 μL of formamide at the following time points: 15 s, 30 s, 1 min, 2 min, 7 min, 10 min, 20 min, 40 min, 1 h, 2 h, 3 h, and 4 h. Quenched reaction products were resolved on 19% denaturing polyacrylamide gels. Gel visualization was done by phosphor screen autoradiography using a STORM840 scanner from Molecular Dynamics. Band intensity quantitation and data plotting were performed with ImageQuant (GE Healthcare) and SigmaPlot 9.0 (Systat Software Inc.), respectively.

Extension from AP Site- and Tg-Containing Base Pairs. Assays examining the ability of Pol X to extend from AP site- and Tg-containing base pairs (where the lesion was in the template strand) were performed in a manner similar to the running-start translesion synthesis assays described above, except that the final concentration of Pol X was increased to 225 nM. Since the activity of the ASFV replicative polymerase opposite to these lesions is not yet known, it was unclear which lesion-containing base pairs Pol X would most likely encounter at primer termini. Accordingly, substrates were designed so as to place either A, T, G, or C (at the primer's 3′ terminus) opposite to either Tg or an AP site in the templating strand (see Table 2 for substrate details).

[4] To achieve a *final* $[Mg^{2+}]_{free}$ of 10 mM, $[Mg^{2+}]_{total}$ was adjusted assuming that the Mg^{2+}·dNTP complex has a K_d of 333 μM.

Fidelity of Nucleotide Incorporation Opposite to 8-Oxo-G in the Template/Primer Context. Fidelity assays were performed in the pre-steady state at 37 °C in the assay buffer described above. Assays were initiated by mixing a protein/DNA solution [consisting of 450 nM Pol X, 200 nM template/primer DNA substrate (which mimics the substrate context that is likely to occur upon stalling of a replisome; see Table 2 for substrate details), 2 mM DTT, and 200 μg/mL BSA] with a dNTP/$MgCl_2$ solution (consisting of varying dNTP concentration and sufficient $MgCl_2$ to achieve a postmixing *free* Mg^{2+} concentration of 10 mM)[4] in a 1:1 ratio. While incorporation of dATP was monitored by rapid chemical quench [quenched using 600 mM Na_2EDTA (pH 8.0)], incorporation of dCTP, dGTP, dTTP, and 7-deaza-dATP was monitored by manually quenching aliquots with formamide. For purposes of comparison, synthesis of the undamaged G·C base pair was monitored by rapid quench under identical conditions using a substrate of identical sequence. All reaction products were resolved and visualized as described above, and data were fit to the single-exponential equation [product] = $A[1 - \exp(-k_{obs}t)]$. The observed rate constants (k_{obs}) thus obtained were plotted as a function of [dNTP] and fit to the hyperbolic equation $k_{obs} = k_{pol}[\text{dNTP}]/(K_{d,app} + [\text{dNTP}])$ to obtain the equilibrium dissociation constant ($K_{d,app}$) and the catalytic rate constant (k_{pol}). The fidelity of nucleotide incorporation was calculated as fidelity = $[(k_{pol}/K_{d,app})_{cor} + (k_{pol}/K_{d,app})_{inc}]/(k_{pol}/K_{d,app})_{inc}$, where the subscripts "cor" and "inc" refer to correct (8-oxo-G·C)[5] and incorrect (8-oxo-G·A, 8-oxo-G·T, 8-oxo-G·G, and 8-oxo-G·deazaA) incorporation, respectively. Saturation curves were typically repeated at least two times; the reported data represent the single best (i.e., highest *R*-squared, coefficient of determination, value) independent trial.

Extension from 8-Oxo-G-Containing Base Pairs. Extension from the 8-oxo-G·A and 8-oxo-G·C base pairs was examined in the pre-steady state in a manner similar to the above assays monitoring incorporation opposite to templating 8-oxo-G; note that, for purposes of comparison, extension from the G·A and G·C base pairs was also examined. Though the nascent templating nucleotide in these extension assays is C (see Table 2 for substrate details), as a preliminary test of dNTP specificity during incorporation at this site, an initial set of time courses simply monitored incorporation of 500 μM dATP, dTTP, dGTP, or dCTP. Subsequently, full saturation curves were generated for synthesis of the C·G base pair at primer termini containing either the G·C, 8-oxo-G·C, G·A, or 8-oxo-G·A base pair.

8-Oxo-dGTP Incorporation Opposite to Undamaged Template. These assays were conducted in the pre-steady state in a manner similar to the above assays monitoring incorporation opposite to templating 8-oxo-G. Both template/primer and single-nucleotide gapped substrates were examined.

RESULTS

Rationale Behind Pol X Assays with Damaged Substrates. Ideally, the ability of a given DNA polymerase to utilize damaged substrates would initially be assessed in vivo by comparing both survival and mutation profiles of WT and polymerase knockout strains in the presence of a given type of lesion. These findings could subsequently be validated and studied in further detail by use of in vitro assays. Because we are presently unable to work with intact ASFV,[3] we used in vitro assays as the starting point in our analysis of Pol X. Since assaying Pol X against each of the myriad known DNA and dNTP lesions would be intractable, ASFV's intracellular microenvironment was taken into consideration to help ascertain which lesions Pol X might most likely encounter. A defining feature of ASFV viral factory formation is the recruitment of host cell mitochondria to encircle clusters of maturing virions (*28*). Since the mitochondria in ASFV viral factories are in an active (as opposed to resting) state of respiration (*29*), and since even under normal conditions oxidative phosphorylation generates reactive oxygen species (ROS) byproducts (*30*) that are capable of diffusing from the mitochondrial matrix into the cytosol, it is conceivable that ASFV may be forced to contend with a high concentration of these harmful radicals.[6] Accordingly, we examined the activity of Pol X against a few of the most common ROS-induced DNA and dNTP lesions.

Qualitative Assessment of Pol X-Catalyzed Lesion Bypass. Pol X was tested for the ability to catalyze translesion synthesis via running-start assays. As shown in Figure 1A, Pol X is incapable of bypassing the oxidative pyrimidine lesion Tg. While a select few polymerases [including yeast Pol ξ (*33*) and human Pols κ (*34*) and η (*35*)] can efficiently bypass Tg, most polymerases are blocked by it, catalyzing the correct incorporation of A opposite the lesion but then being incapable of extending from the Tg·A primer terminus (*36*−*40*). In contrast, Pol X pauses one nucleotide upstream of Tg, effecting diminutive incorporation opposite the lesion itself. However, this high level of discrimination does not encompass all ring-saturated pyrimidines since Pol X is capable of bypassing DHT, albeit with slightly reduced efficiency; Figure 1B shows that though incorporation directly opposite to DHT is hindered relative to the undamaged control substrate (as evidenced by the accumulation of the 19mer species in the gel), once incorporation has occurred opposite to DHT, extension beyond the lesion proceeds uninhibited. In support of a bypass mechanism involving direct incorporation opposite to DHT (rather than a −1 "deletion" frameshift mechanism wherein the lesion is extruded from the helix and the adjacent 5′ nucleotide serves as template for the incoming dNTP) are the facts that (i) the total number of bands in Figure 1B is consistent with the size of the 45mer substrate and (ii) the location of pause sites "downstream" of the lesion matches the location of pause sites in the control substrate (if a frameshift mechanism had been employed, the pause sites in the DHT and control substrates would not line up with one another).

[5] In the base pair notation X·Y, X refers to the templating position and Y denotes the incoming dNTP.

[6] Others have made general statements suggesting that because ASFV inhabits macrophages, it is necessarily exposed to a highly oxidative environment (*31*). Upon phagocytosis of a virus or bacterium, macrophages effect an oxidative burst wherein ROS are generated inside the phagolysosome to inactivate the pathogen. Since ASFV gains access to the cytosol via receptor-mediated endocytosis (*32*), the oxidative burst does not appear to be relevant to ASFV.

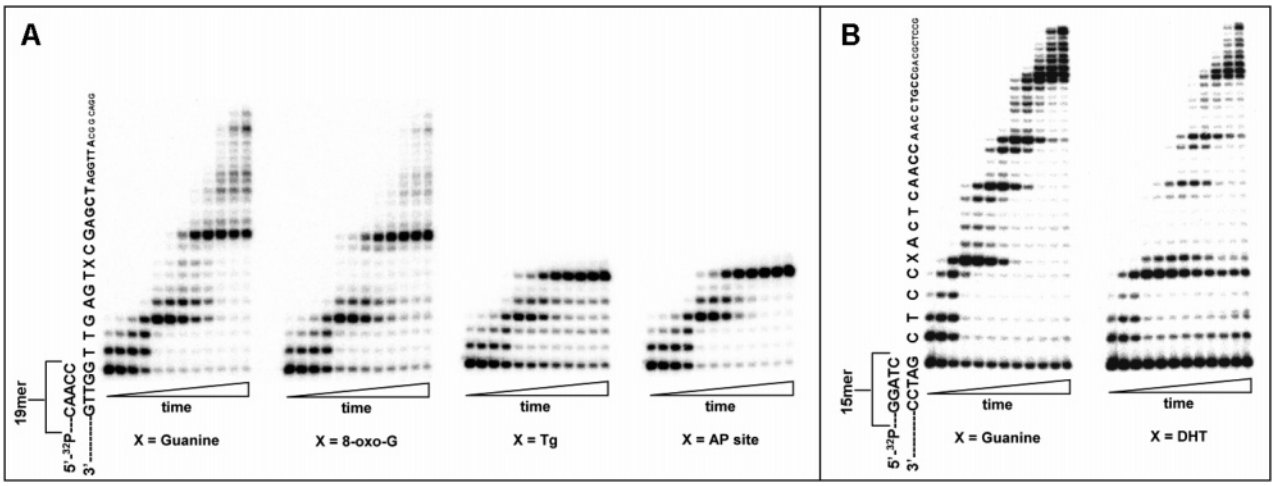

FIGURE 1: Pol X-catalyzed translesion synthesis. (A) Comparison of templating guanine vs templating 8-oxo-G, Tg, and an AP site. The running-start substrate, displayed such that each nucleotide position aligns with its corresponding band in the gels, allows for multiple nucleotides to be incorporated prior to encountering the lesion. For each individual assay the lanes, from left to right, correspond to time points of 15 s, 30 s, 1 min, 2 min, 7 min, 10 min, 20 min, 40 min, 1 h, 2 h, 3 h, and 4 h. (B) Comparison of templating guanine vs DHT. These assays were similar to those described above in (A), except that the running-start substrate was different both in sequence *and* in the position of the lesion.

Unlike its closest homologue eukaryotic Pol β, which bypasses AP sites by both direct incorporation and misalignment mechanisms (*41*), Pol X is entirely blocked by this lesion, catalyzing incorporation opposite the preceding templating position but showing minimal incorporation opposite the lesion itself (Figure 1A). Considering the structurally distinct mechanisms by which Pol β and Pol X bind single-nucleotide gapped substrate (*12*, *42*), the different capacity for AP site bypass displayed by these orthologues is not surprising.

Consistent with what has been observed for a large number of diverse polymerases (*43*−*45*), Pol X incorporates opposite to/extends beyond the common oxidative purine lesion 8-oxo-G (Figure 1A). Unlike the reduced efficiency it showed while incorporating opposite to DHT, Pol X appears to bypass 8-oxo-G as efficiently as the undamaged control substrate.

Qualitative Assessment of Extension from AP Site- and Tg-Containing Primer Termini. The inability of Pol X to incorporate opposite to Tg and the AP site (Figure 1A) does not necessarily indicate that it could not contribute to bypass of these lesions. A number of polymerases with complementary properties have been shown to effect translesion synthesis by working in tandem: while the first polymerase incorporates opposite to the lesion but cannot subsequently extend the lesion-containing primer terminus, a second polymerase efficiently extends the lesion-containing primer terminus but is incapable of incorporating directly opposite to the lesion. Examples include the sequential action of Pols η and ξ on pyrimidine (6-4) pyrimidone photoproducts (*46*) and the sequential action of Pols δ and κ on O^6-methylguanine (*22*).

Assuming that the ASFV replicative polymerase could incorporate opposite to Tg and an AP site, we tested whether Pol X might subsequently be capable of extending these lesion-containing primer termini. We found that Pol X is incapable of extending from primer termini that contain either an abasic site or Tg in the templating strand; this inhibition is observed regardless of which nucleotide (A, T, G, or C) is located opposite the lesion (data not shown; see Table 2 for substrate details).

dNTP Preference Opposite to Templating 8-Oxo-G in the Template/Primer Context. Because 8-oxo-G readily assumes a *syn* conformation about its glycosidic bond (*47*) (to avoid steric clashing with the sugar−phosphate backbone), it has a heightened capacity for using its Hoogsteen face to hydrogen bond with incoming dATP (Figure 2A). The extent to which the 8-oxo-G·A mismatch is favored over the 8-oxo-G·C "match" varies from one polymerase to the next and with DNA sequence context (*43*−*45*, *48*, *49*). To examine the mutagenic potential of templating 8-oxo-G when copied by Pol X, pre-steady state incorporation assays were performed (Figure 3) using a template/primer substrate with the lesion in the nascent templating position (Table 2); this substrate likely mimics what Pol X would encounter if it were to "rescue" the ASFV replicative polymerase stalled at 8-oxo-G.

As shown in Table 3, Pol X incorporates A and C opposite to 8-oxo-G much more efficiently than it incorporates T and G opposite the lesion, suggesting that, like many polymerases, Pol X readily accommodates both the *syn* (8-oxo-G·A) and the *anti* (8-oxo-G·C) conformations of templating 8-oxo-G (Figure 2A). Discrimination against incoming dTTP and dGTP is achieved primarily through the k_{pol} parameter, the average k_{pol} for dTTP and dGTP being ~190-fold lower than the average k_{pol} for dATP and dCTP. Because it synthesizes the 8-oxo-G·A mismatch 2-fold more efficiently than 8-oxo-G·C, if Pol X does in fact encounter this lesion in vivo, G·C → T·A transversion mutations will frequently occur. Note that Pol X synthesizes 8-oxo-G·A slightly more efficiently than the nondamaged G·C base pair; to our knowledge this is unique among polymerases.

8-Oxo-G·A Synthesis: Analysis of dATP Conformation. As stated above, that Pol X is adept at synthesizing the 8-oxo-G·A base pair is strong evidence that the Hoogsteen face of 8-oxo-G is being employed. However, the base pairing scheme illustrated in Figure 2A is not the only possibility: dATP could also use its Hoogsteen face to hydrogen bond

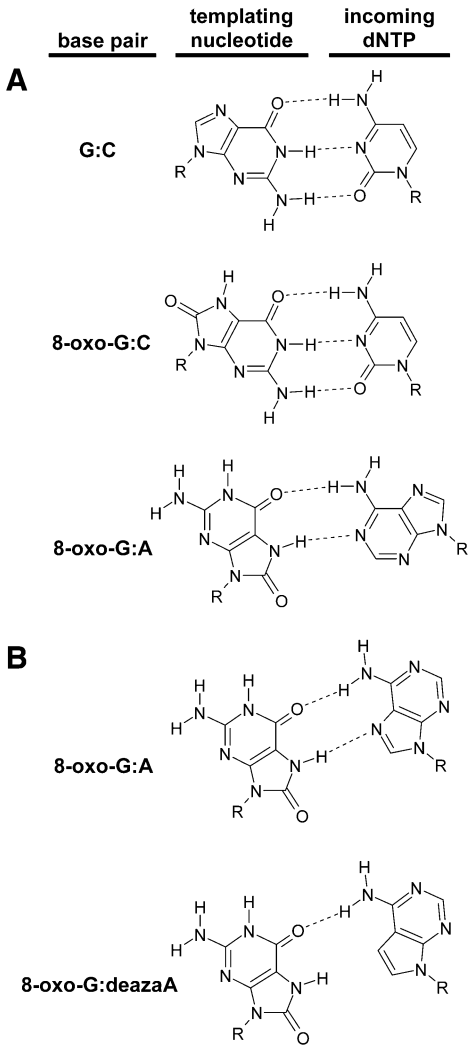

FIGURE 2: Base pairing schemes involving guanine or 8-oxoguanine in the templating strand. (A) Dual coding potential of 8-oxo-G. Note that whereas 8-oxo-G utilizes its Watson−Crick face to base pair with incoming dCTP, it utilizes its Hoogsteen face to base pair with incoming dATP. (B) Examining the conformation of incoming dATP opposite to templating 8-oxo-G. While incoming dATP can use its Watson−Crick face to base pair with templating 8-oxo-G [as shown above in (A)], it can also utilize its Hoogsteen face. The importance of the Hoogsteen face of dATP can be evaluated using the analogue 7-deaza-dATP.

with the Hoogsteen face of 8-oxo-G (Figure 2B). To shed further light on the conformation/geometry of the 8-oxo-G·A base pair in the active site of Pol X, incorporation of 7-deaza-dATP opposite to 8-oxo-G was monitored. As shown in Table 3, the catalytic efficiency for synthesis of the 8-oxo-G·deazaA base pair is actually slightly higher than that for 8-oxo-G·A. That loss of the N^7 hydrogen bond acceptor in the incoming nucleotide is not deleterious suggests that the Hoogsteen face of dATP is not utilized and that the 8-oxo-G·A base pair almost certainly has the conformation shown in Figure 2A rather than that shown in Figure 2B.

Extension from 8-Oxo-G-Containing Base Pairs. The apparent absence of pausing downstream of the 8-oxo-G lesion in the TLS assay of Figure 1A suggests that, at least in this sequence context, Pol X is adept at extending from an 8-oxo-G-containing base pair. To test, quantitatively, how the presence of this lesion at the primer terminus affects the activity and fidelity of Pol X, pre-steady state assays were employed. Because Pol X incorporates A and C opposite to 8-oxo-G preferentially, analyses were focused on extension from the 8-oxo-G·A and 8-oxo-G·C base pairs; for purposes of comparison, extension from the G·A and G·C base pairs was also examined. Because the presence of 8-oxo-G in the primer's 3′-terminal base pair could conceivably alter fidelity during primer extension, Pol X's dNTP specificity during lesion extension was first examined by simply monitoring incorporation of 500 μM dATP, dTTP, dGTP, or dCTP (Table 4). The nascent templating position in these extension assays is C. Consistent with this, Pol X preferentially incorporates G regardless of the identity of the base pair at the primer terminus.

In light of the above, we next generated pre-steady state saturation curves for synthesis of C·G when the base pair at the primer terminus was either 8-oxo-G·A (using G·A as a control) or 8-oxo-G·C (using G·C as a control). The data, which are displayed in Table 5, indicate the following. (i) Relative to undamaged G, the presence of 8-oxo-G in the templating position of the primer's 3′-terminal base pair has little impact on Pol X's affinity for incoming nucleotide: the $K_{d,app}$ for the C·G base pair being synthesized is 17, 17, and 15 μM when the primer's 3′-terminal base pair is 8-oxo-G·C, G·C, or 8-oxo-G·A, respectively. (ii) Similarly, relative to undamaged G, the presence of 8-oxo-G in the templating position of the primer's 3′-terminal base pair does not significantly perturb k_{pol}. (iii) When combined, the above properties result in Pol X extending the 8-oxo-G·C and 8-oxo-G·A base pairs slightly more efficiently than the G·C base pair. (iv) Relative to extension from the 8-oxo-G·A base pair, extension from the G·A mismatch is associated with a 15-fold enhancement in affinity for incoming nucleotide and a 214-fold reduction in k_{pol}. Collectively, this results in a 14-fold decrease in catalytic efficiency. In contrast, the difference in the catalytic efficiencies for extension of the G·C and 8-oxo-G·C base pairs is just 1.6-fold. While the 8-oxo-G·C and G·C base pairs are both expected to exist in the canonical Watson−Crick geometry (Figure 2A), the Hoogsteen geometry that facilitates 8-oxo-G·A formation is not expected to be utilized in the G·A base pair. The difference in the efficiency of extension from 8-oxo-G·A vs G·A would therefore seem to be best explained by this qualitative difference in base pair geometry.

Incorporation of 8-Oxo-dGTP. Since the conditions that produce 8-oxo-G within a DNA duplex are also capable of converting dGTP into 8-oxo-dGTP, and since ASFV does not appear to encode a nudix hydrolase that is specific for cleansing the nucleotide pool of this damaged substrate (*50*), it seemed worthwhile to examine the ability of Pol X to utilize, or discriminate against, this nucleotide. Pre-steady state incorporation of 8-oxo-dGTP opposite to either C or A in the context of both a template/primer and a single-nucleotide gap was monitored (Figure 4 and Table 6); since preliminary analyses indicated that incorporation of 8-oxo-dGTP opposite to templating T and G is extremely inefficient (data not shown), these templates were not examined quantitatively.

(A) Single-Nucleotide Gap Context. As shown in Table 6, the catalytic efficiency for synthesis of the C·8-oxo-G and A·8-oxo-G base pairs is reduced 780-fold and 1560-fold, respectively, compared to the Watson−Crick C·G base pair. This discrimination against incorporation of the damaged nucleotide is accomplished by both a reduced k_{pol} (5−8-fold

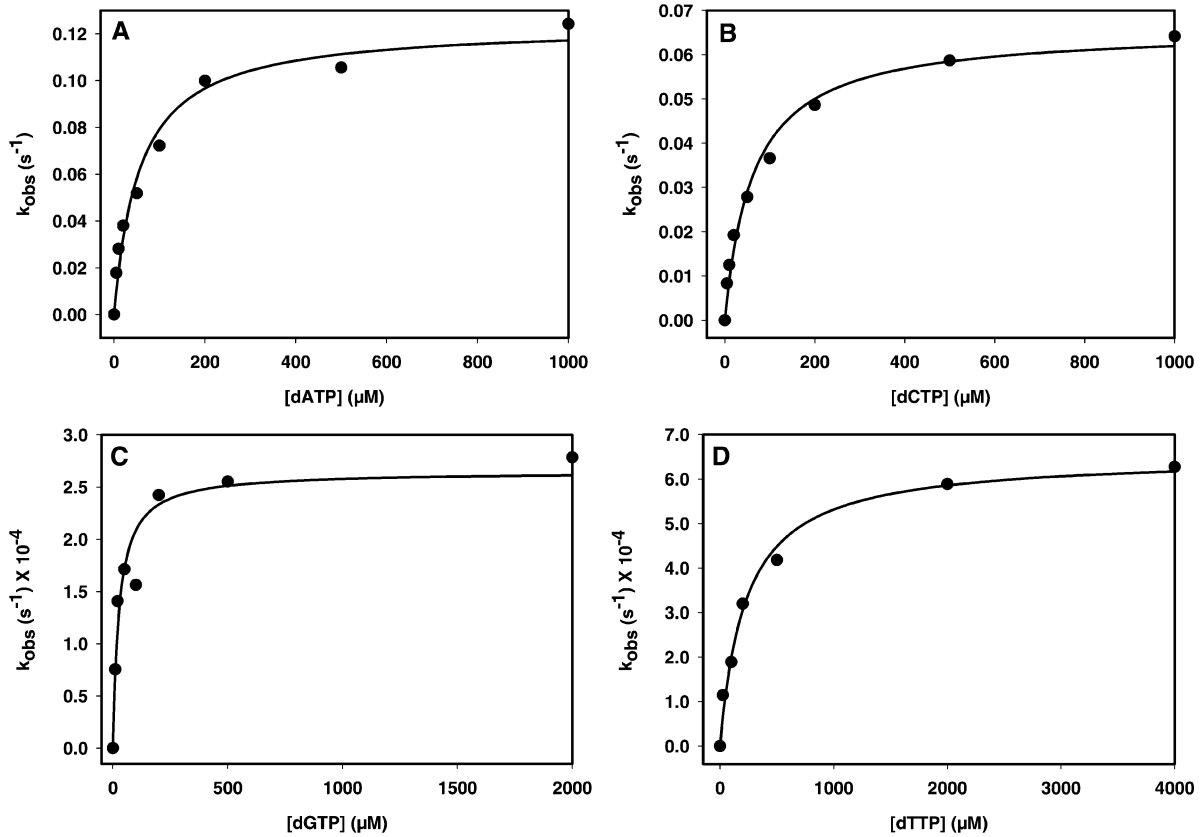

FIGURE 3: Saturation curves for Pol X-catalyzed nucleotide incorporation opposite to 8-oxo-G in a template/primer context. The incoming nucleotide was dATP (A), dCTP (B), dGTP (C), or dTTP (D). Observed rate constants are plotted as a function of the incoming nucleotide concentration; data points (●) are fit to a hyperbola. Kinetic parameters are listed in Table 3.

Table 3: Kinetic Parameters for Pol X-Catalyzed Pre-Steady State Single-Nucleotide Incorporation Opposite to 8-Oxo-G in the Template/Primer Context

base pair[a]	k_{pol} (s^{-1})	$K_{d,app}$ (μM)	$k_{pol}/K_{d,app}$ (M^{-1} s^{-1})	fidelity[b]
8-oxo-G·A	0.12 ± 0.01	56 ± 10	2100	1.5
8-oxo-G·deazaA	0.079 ± 0.001	16 ±1	4900	1.2
8-oxo-G·C	0.066 ± 0.003	63 ± 9	1000	
8-oxo-G·G	0.00030 ± 0.00002	27 ± 8	11	92
8-oxo-G·T	0.00070 ± 0.00002	230 ± 30	3.0	330
G·C[c]	0.059 ± 0.004	39 ± 10	1500	

[a] In the base pair notation X·Y, X refers to the templating position, and Y denotes the incoming nucleotide. [b] Fidelity is defined here as $[(k_{pol}/K_{d,app})_{cor} + (k_{pol}/K_{d,app})_{inc}]/(k_{pol}/K_{d,app})_{inc}$, where the subscripts "cor" and "inc" refer to correct (8-oxo-G·C) and incorrect (8-oxo-G·A, 8-oxo-G·deazaA, 8-oxo-G·T, and 8-oxo-G·G) incorporation, respectively. [c] Incorporation of C opposite to undamaged templating G.

Table 4: Pre-Steady-State Rate Constants (k_{obs}) for Pol X-Catalyzed Extension from 8-Oxo-G-Containing Base Pairs in the Presence of 500 μM Incoming dNTP

base pair[a] at primer terminus	base pair[a] being synthesized[b]			
	C·G	C·T	C·C	C·A
8-oxo-G·A	4.5	0.039	0.0012	0.0048
8-oxo-G·C	2.1	0.013	0.0003	0.0004
G·A	0.0067	0.0017	0.0036	0.0004
G·C	1.4	0.0081	0.0002	0.0003

[a] In the base pair notation X·Y, X refers to the nucleotide in the templating strand, and Y denotes either the nucleotide at the primer's 3′ terminus or the nucleotide that is presently being incorporated. [b] k_{obs} values have units of min^{-1}.

Table 5: Kinetic Parameters for Pol X-Catalyzed Pre-Steady-State Extension from 8-Oxo-G-Containing Base Pairs

base pair[a] at primer terminus	base pair[a] being synthesized	k_{pol} (s^{-1})	$K_{d,app}$ (μM)	$k_{pol}/K_{d,app}$ (M^{-1} s^{-1})
8-oxo-G·C	C·G	0.025 ± 0.001	17 ± 2	1500
G·C	C·G	0.016 ± 0.001	17 ± 3	940
8-oxo-G·A	C·G	0.047 ± 0.003	15 ± 3	3100
G·A	C·G	0.00022 ± 0.00001	1.0 ± 0.2	220

[a] In the base pair notation X·Y, X refers to the nucleotide in the templating strand, and Y denotes either the nucleotide at the primer's 3′ terminus or the nucleotide that is presently being incorporated.

reduction) and a dramatic reduction in binding affinity ($K_{d,app}$ increases ~160−190-fold). While similar means of discriminating against 8-oxo-dGTP have been described for a large number of polymerases (*53*, *54*), these other enzymes typically achieve even greater selectivity against the damaged nucleotide, displaying $(k_{cat}/K_M)_{C\cdot G}/(k_{cat}/K_M)_{C\cdot 8-oxo-G}$ ratios on the order of 10^4-10^6 vs 10^2-10^3 displayed by Pol X.

(B) Template/Primer Context. Relative to the use of single-nucleotide gapped substrate, on a template/primer substrate Pol X incorporates 8-oxo-dGTP with slightly higher affinity but with a slightly lower rate constant. The most important finding from the template/primer substrate in Table 6 is derived from comparison with the data for incorporation *opposite to* 8-oxo-G in Table 3: Pol X is dramatically more tolerant of 8-oxo-G in the templating position than it is in the incoming nucleotide (i.e., Pol X's ability to utilize 8-oxo-G is asymmetric). In the template/primer context, using substrates that are identical in sequence, Pol X synthesizes

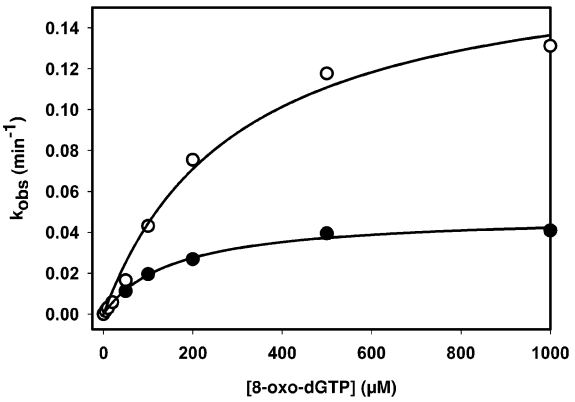

FIGURE 4: Saturation curves for Pol X-catalyzed incorporation of 8-oxo-dGTP in the template/primer context. The templating nucleotide was either A (●) or C (○). Observed rate constants are plotted as a function of 8-oxo-dGTP concentration and fit to a hyperbola. Kinetic parameters are listed in Table 6.

Table 6: Kinetic Parameters for Pol X-Catalyzed Pre-Steady State Incorporation of 8-Oxo-dGTP into Template/Primer or Single-Nucleotide Gapped Substrate

substrate type	base pair[a]	k_{pol} (s^{-1})	$K_{d,app}$ (μM)	$k_{pol}/K_{d,app}$ (M^{-1} s^{-1})
gapped	C·G	0.023 ± 0.001	4.6 ± 0.9	5000
gapped	C·8-oxo-G	0.0046 ± 0.0003	720 ± 80	6.4
gapped	A·8-oxo-G	0.0028 ± 0.0001	880 ± 70	3.2
template/primer	C·8-oxo-G	0.0030 ± 0.0002	300 ± 50	10
template/primer	A·8-oxo-G	0.00081 ± 0.00002	150 ± 10	5.4

[a] In the base pair notation X·Y, X refers to the templating position, and Y denotes the incoming nucleotide.

8-oxo-G·A 390-fold more efficiently than A·8-oxo-G and synthesizes 8-oxo-G·C 100-fold more efficiently than C·8-oxo-G. Collectively, this indicates that Pol X, in the context of the 8-oxo-G lesion, can accommodate a Hoogsteen (i.e., *syn*) conformation in the templating base, but not in the incoming nucleotide. Note that this is consistent with the above finding that the Hoogsteen face of incoming dATP is not important during synthesis of the 8-oxo-G·A base pair (Table 3 and Figure 2).

DISCUSSION

Utilization of Damaged Substrates by Pol X and the Biological Implications Thereof. (A) Tg and DHT. Pol X's total blockage by Tg and efficient usage of DHT (Figure 1) are consistent both with what has been observed for other polymerases and with the extensive and minor, respectively, local structural perturbations associated with these lesions (*55*, *56*). While DHT was experimentally useful for purposes of comparison with Tg, the fact that DHT is formed preferentially under anoxic conditions (*57*) suggests that it is probably not very relevant to ASFV. Tg, on the other hand, is a common lesion in an oxygenated environment (*58*) and may be a particularly important form of damage in ASFV viral factories due to the large number of respiring mitochondria that are found in close proximity to viral genomes (*28*). Considering the fact that the replicative polymerases which the ASFV replicative polymerase shows homology to are significantly inhibited by Tg (at both the incorporation and extension steps) (*35*, *40*), that Pol X is entirely blocked by Tg, that ASFV does not encode any DNA glycosylases (*3*), and that there is presently no evidence for the recruitment of host DNA repair factors by ASFV, it would appear that Tg is likely to be either lethal or highly deleterious in the ASFV genome.

(B) AP Sites. While some polymerases are incapable of bypassing AP sites, others bypass the lesion via frameshift mechanisms, and still others are capable of incorporating directly opposite the lesion. Considering its high tolerance for synthesizing mismatched base pairs of diverse size/geometry (G·G and T·T, for example) (*9*), it is intriguing that Pol X shows an absolute requirement for the presence of a templating base (Figure 1A). It is not yet known whether the ASFV replicative polymerase can bypass AP sites, but even if it is blocked, AP sites in the viral genome are probably not as pernicious as Tg because the ASFV DNA repair system (consisting of APE, Pol X, and DNA ligase) is capable of processing them (*8*).

(C) 8-Oxo-G. Whether Pol X would have the opportunity to facilitate bypass of 8-oxo-G in a template/primer context is unclear. Though the ASFV replicative polymerase has been described as a homologue of both human Pol α and human Pol δ[7] (*59*, *60*), it is unique from other viral Pol α-like enzymes in its complete resistance to the inhibitor aphidicolin (*61*). While Pol α-like enzymes bypass 8-oxo-G efficiently (*48*, *62*, *63*), Pol δ is significantly inhibited both during incorporation opposite the lesion and during extension of the lesion-containing base pair (*44*). Accordingly, the ability of the ASFV replicative polymerase to bypass 8-oxo-G cannot be predicted with confidence. If it is blocked or inhibited by this lesion, Pol X could clearly facilitate bypass (Figure 1A and Tables 3−5) and would, because of its preferential incorporation of A opposite to the lesion, frequently generate G·C → T·A transversion mutations. That it both synthesizes and subsequently extends from the 8-oxo-G·A base pair with relatively high efficiency suggests that Pol X readily accommodates the *syn* rotamer of the oxidized base when it is located both at the nascent templating position and in the terminal base pair of the primer, respectively.

(D) 8-Oxo-dGTP. Though it was initially suggested that ASFV encodes a MutT (a nudix hydrolase responsible for cleansing the nucleotide pool of 8-oxo-dGTP) homologue (*3*), this gene was subsequently shown to be most similar to the diadenosine tetraphosphate hydrolases, with the protein hydrolyzing diphosphoinositol polyphosphates preferentially (*50*). Thus, unless ASFV recruits a MutT-like activity from the host cell, 8-oxo-dGTP could conceivably be present in the mitochondria-rich ASFV viral factories at elevated concentrations.

Most polymerases discriminate against incoming 8-oxo-dGTP very strongly, displaying discrimination factors [$(k_{cat}/K_M)_{C\cdot G}/(k_{cat}/K_M)_{C\cdot 8-oxo-G}$] in the range of 10^4-10^6 (*53*, *54*). In contrast, Pol X favors incoming dGTP over 8-oxo-dGTP by a factor of only 7.8×10^2 (Table 6). The only other polymerases known to be so accommodating of incoming 8-oxo-dGTP are MLV RT [discrimination factor = 1.8×10^2 (*54*)] and eukaryotic Pol β [discrimination factor = 1.4

[7] We find the ASFV replicative polymerase (AAA65319) to display 22% and 23% similarity to the catalytic subunit of human Pols α (P09884) and δ (P28340), respectively. The numbers listed in parentheses are the NCBI accession numbers.

$\times 10^2-3.9 \times 10^2$ (*54*, *64*)]. However, unlike Pol β which incorporates 8-oxo-dGTP opposite to templating A 24-fold more efficiently than opposite to templating C (*64*), Pol X preferentially incorporates the damaged nucleotide opposite to C (2-fold more efficiently than opposite to A).

Despite its *relatively* efficient usage of 8-oxo-dGTP, the minimal number of incorporation events that Pol X is expected to catalyze per genome [since it is a repair or perhaps a TLS, not a replicative, polymerase (*9*, *51*, *52*)] suggests that 8-oxo-G is probably not incorporated very frequently. Once incorporated into a single-nucleotide gap, persistence of 8-oxo-G in the genome would be dependent upon the relative efficiencies of the competing reactions catalyzed by ASFV APE (removal of 8-oxo-G via its 3′ → 5′ exonuclease editing activity)[8] and ASFV DNA ligase (sealing the 8-oxo-G-containing nick to give a stable, contiguous duplex).[9]

TLS Activity and Error-Proneness in Pol X. The objective of the work described here was to obtain clues that could help to explain why ASFV Pol X has evolved to be one of the most error-prone DNA polymerases known. The mutagenic ASFV DNA repair pathway that we previously hypothesized, in which Pol X is the driving mutator force, is consistent with biological data for the virus. Of particular importance to this hypothesis are the facts that (i) the ASFV-encoded AP endonuclease is essential for viral viability when wild isolates of ASFV are passaged in macrophages (the native host cell) but not when the Vero cell-adapted BA71V strain of ASFV is passaged in Vero cells (*31*), suggesting that the extent of viral genome damage is more extensive in macrophages than it is in Vero cells, and (ii) ASFV field isolates passaged in porcine macrophages display greater antigenic diversification than does the Vero cell-adapted BA71V strain after passage in Vero cells (*14*). A straightforward explanation for these findings is that the ASFV DNA "repair" system has more extensive access to the viral genome in macrophage cells and therefore has greater opportunity to effect mutagenesis. Alternatively, the enhanced diversification of viral antigens that is observed in macrophages could also be due to a greater extent of error-prone translesion DNA synthesis catalyzed by Pol X and/or the ASFV replicative DNA polymerase. Since replicative polymerases of the α and δ types (which the ASFV replicative polymerase is most similar to) are not typically robust in TLS activity (*15*), and since Pol X is similar to many TLS polymerases in its extreme error-proneness when copying undamaged templates (*9*, *10*), the possibility that Pol X may have been selected for TLS activity seemed worthy of investigation. What do our results suggest regarding this possibility?

The activities that Pol X displays against damaged DNA and dNTP substrates are rather pedestrian: inhibition by Tg and AP sites, bypass of DHT and 8-oxo-G, and discrimination against 8-oxo-dGTP are properties common to many polymerases. While Pol X is unique in its slight preference of 8-oxo-G·A over G·C, and in its relatively weak discrimination against incoming 8-oxo-dGTP, neither of these properties are so dramatic in their magnitude as to suggest that they represent strong selection criteria in the evolution of this enzyme. While these preliminary findings suggest that the property of error-proneness on undamaged substrates may be uniquely decoupled from TLS activity in Pol X, the lesions examined here admittedly represent only a fraction of the DNA/dNTP lesions that are presently known. Further examination of TLS activity in Pol X therefore seems warranted, albeit with the caveat provided below.

Biological data regarding the specific types of DNA/dNTP damage encountered during the replication/assembly of the ASFV genome are presently not available, forcing us to make educated guesses based on the microenvironment of ASFV viral factories. Even if the large numbers of respiring mitochondria in ASFV viral factories do not give rise to an increased concentration of ROS (as we have hypothesized), ASFV is still expected to be subject to "background" levels of ROS; accordingly, the oxidative lesions examined here seem to be the most reasonable starting point. However, it is possible that the DNA and dNTP lesions we have examined are not the most abundant or pernicious types of damage sustained by ASFV in its native environment. While further in vitro analyses of the type employed here could potentially identify a lesion which Pol X shows high activity/specificity for, biological data will be critical for guiding future efforts in order to avoid a simple "shooting in the dark" scenario. Moreover, in vivo data will be essential for establishing biological relevance (since TLS activities identified in vitro are not necessarily important in vivo).

Though data were not actually provided, Blanco and coworkers have indicated that Pol X is not expressed until the later stages of ASFV infection (*52*), whereas the ASFV replicative polymerase is expressed at both early and late stages of infection (*59*, *60*). It would therefore appear that if Pol X is indeed involved in TLS, it shows up at the last minute to rescue severely hindered replisomes. An alternative explanation for the late expression of Pol X is that it is involved in the repair (and, perhaps, mutagenesis) of what are essentially complete, but damaged, genomes immediately prior to their being packaged into viral capsids. Both TLS and mutagenic DNA repair would represent, to our knowledge, unique features of viral genome processing. It is hoped that the questions, data, and discussion presented here will prompt in vivo analyses (by those with access to the virus) that elucidate, in detail, the specific contributions that Pol X makes to ASFV fitness/adaptability.

[8] Human Ape1 and *S. cerevisiae* Apn1, which are homologues of ASFV APE, have both been shown to efficiently remove 8-oxo-G from the 3′ side of a nick (*65*).

[9] To our knowledge, the efficiency of ligating nicks containing oxidatively damaged nucleotides has not previously been examined.

REFERENCES

1. Vinuela, E. (1985) African swine fever virus, *Curr. Top. Microbiol. Immunol. 116*, 151−170.
2. Blasco, R., Aguero, M., Almendral, J. M., and Vinuela, E. (1989) Variable and constant regions in African swine fever virus DNA, *Virology 168*, 330−338.
3. Yanez, R. J., Rodriguez, J. M., Nogal, M. L., Yuste, L., Enriquez, C., Rodriguez, J. F., and Vinuela, E. (1995) Analysis of the complete nucleotide sequence of African swine fever virus, *Virology 208*, 249−278.
4. Enjuanes, L., Cubero, I., and Vinuela, E. (1977) Sensitivity of macrophages from different species to African swine fever (ASF) virus, *J. Gen. Virol. 34*, 455−463.
5. Garcia-Beato, R., Salas, M. L., Vinuela, E., and Salas, J. (1992) Role of the host cell nucleus in the replication of African swine fever virus DNA, *Virology 188*, 637−649.

6. Brookes, S. M., Dixon, L. K., and Parkhouse, R. M. (1996) Assembly of African Swine fever virus: quantitative ultrastructural analysis in vitro and in vivo, *Virology 224*, 84−92.
7. Rojo, G., Garcia-Beato, R., Vinuela, E., Salas, M. L., and Salas, J. (1999) Replication of African swine fever virus DNA in infected cells, *Virology 257*, 524−536.
8. Lamarche, B. J., and Tsai, M.-D. (2006) Contributions of an endonuclease IV homologue to DNA repair in the African swine fever virus, *Biochemistry 45*, 2790−803.
9. Showalter, A. K., and Tsai, M.-D. (2001) A DNA polymerase with specificity for five base pairs, *J. Am. Chem. Soc. 123*, 1776−1777.
10. Lamarche, B. J., Kumar, S., and Tsai, M.-D. (2006) ASFV DNA polymerase X is extremely error-prone under diverse assay conditions and within multiple DNA sequence contexts, *Biochemistry 45*, 14826−14833.
11. Lamarche, B. J., Showalter, A. K., and Tsai, M.-D. (2005) An error-prone viral DNA ligase, *Biochemistry 44*, 8408−8417.
12. Showalter, A. K., Byeon, I. J., Su, M. I., and Tsai, M.-D. (2001) Solution structure of a viral DNA polymerase X and evidence for a mutagenic function, *Nat. Struct. Biol. 8*, 942−946.
13. Dixon, L. K., and Wilkinson, P. J. (1988) Genetic diversity of African swine fever virus isolates from soft ticks (*Ornithodoros moubata*) inhabiting warthog burrows in Zambia, *J. Gen. Virol. 69* (Part 12), 2981−2993.
14. Garcia-Barreno, B., Sanz, A., Nogal, M. L., Vinuela, E., and Enjuanes, L. (1986) Monoclonal antibodies of African swine fever virus: antigenic differences among field virus isolates and viruses passaged in cell culture, *J. Virol. 58*, 385−392.
15. Rattray, A. J., and Strathern, J. N. (2003) Error-prone DNA polymerases: when making a mistake is the only way to get ahead, *Annu. Rev. Genet. 37*, 31−66.
16. Tippin, B., Pham, P., and Goodman, M. F. (2004) Error-prone replication for better or worse, *Trends Microbiol. 12*, 288−295.
17. Shcherbakova, P. V., and Fijalkowska, I. J. (2006) Translesion synthesis DNA polymerases and control of genome stability, *Front. Biosci. 11*, 2496−2517.
18. Yeiser, B., Pepper, E. D., Goodman, M. F., and Finkel, S. E. (2002) SOS-induced DNA polymerases enhance long-term survival and evolutionary fitness, *Proc. Natl. Acad. Sci. U.S.A. 99*, 8737−8741.
19. Johnson, R. E., Prakash, S., and Prakash, L. (1999) Efficient bypass of a thymine-thymine dimer by yeast DNA polymerase, Poleta, *Science 283*, 1001−1004.
20. Vaisman, A., Frank, E. G., Iwai, S., Ohashi, E., Ohmori, H., Hanaoka, F., and Woodgate, R. (2003) Sequence context-dependent replication of DNA templates containing UV-induced lesions by human DNA polymerase iota, *DNA Repair (Amsterdam) 2*, 991−1006.
21. Zhang, Y., Wu, X., Guo, D., Rechkoblit, O., Taylor, J. S., Geacintov, N. E., and Wang, Z. (2002) Lesion bypass activities of human DNA polymerase mu, *J. Biol. Chem. 277*, 44582−44587.
22. Haracska, L., Prakash, L., and Prakash, S. (2002) Role of human DNA polymerase kappa as an extender in translesion synthesis, *Proc. Natl. Acad. Sci. U.S.A. 99*, 16000−16005.
23. Johnson, R. E., Washington, M. T., Haracska, L., Prakash, S., and Prakash, L. (2000) Eukaryotic polymerases iota and zeta act sequentially to bypass DNA lesions, *Nature 406*, 1015−1019.
24. Nair, D. T., Johnson, R. E., Prakash, S., Prakash, L., and Aggarwal, A. K. (2004) Replication by human DNA polymerase-iota occurs by Hoogsteen base-pairing, *Nature 430*, 377−380.
25. Nair, D. T., Johnson, R. E., Prakash, L., Prakash, S., and Aggarwal, A. K. (2006) An incoming nucleotide imposes an anti to syn conformational change on the templating purine in the human DNA polymerase-iota active site, *Structure 14*, 749−755.
26. Uljon, S. N., Johnson, R. E., Edwards, T. A., Prakash, S., Prakash, L., and Aggarwal, A. K. (2004) Crystal structure of the catalytic core of human DNA polymerase kappa, *Structure 12*, 1395−1404.
27. Ling, H., Boudsocq, F., Plosky, B. S., Woodgate, R., and Yang, W. (2003) Replication of a cis-syn thymine dimer at atomic resolution, *Nature 424*, 1083−1087.
28. Rojo, G., Chamorro, M., Salas, M. L., Vinuela, E., Cuezva, J. M., and Salas, J. (1998) Migration of mitochondria to viral assembly sites in African swine fever virus-infected cells, *J. Virol. 72*, 7583−7588.
29. Rojo, G., Chamorro, M., Salas, M. L., Vinuela, E., Cuezva, J. M., and Salas, J. (1998) Migration of mitochondria to viral assembly sites in African swine fever virus-infected cells, *J. Virol. 72*, 7583−7588.
30. Beckman, K. B., and Ames, B. N. (1998) The free radical theory of aging matures, *Physiol. Rev. 78*, 547−581.
31. Redrejo-Rodriguez, M., Garcia-Escudero, R., Yanez-Munoz, R. J., Salas, M. L., and Salas, J. (2006) African swine fever virus protein pE296R is a DNA repair apurinic/apyrimidinic endonuclease required for virus growth in swine macrophages, *J. Virol. 80*, 4847−4857.
32. Alcami, A., Carrascosa, A. L., and Vinuela, E. (1990) Interaction of African swine fever virus with macrophages, *Virus Res. 17*, 93−104.
33. Johnson, R. E., Yu, S. L., Prakash, S., and Prakash, L. (2003) Yeast DNA polymerase zeta (zeta) is essential for error-free replication past thymine glycol, *Genes Dev. 17*, 77−87.
34. Fischhaber, P. L., Gerlach, V. L., Feaver, W. J., Hatahet, Z., Wallace, S. S., and Friedberg, E. C. (2002) Human DNA polymerase kappa bypasses and extends beyond thymine glycols during translesion synthesis in vitro, preferentially incorporating correct nucleotides, *J. Biol. Chem. 277*, 37604−37611.
35. Kusumoto, R., Masutani, C., Iwai, S., and Hanaoka, F. (2002) Translesion synthesis by human DNA polymerase eta across thymine glycol lesions, *Biochemistry 41*, 6090−6099.
36. Ide, H., Kow, Y. W., and Wallace, S. S. (1985) Thymine glycols and urea residues in M13 DNA constitute replicative blocks in vitro, *Nucleic Acids Res. 13*, 8035−8052.
37. Rouet, P., and Essigmann, J. M. (1985) Possible role for thymine glycol in the selective inhibition of DNA synthesis on oxidized DNA templates, *Cancer Res. 45*, 6113−6118.
38. Hayes, R. C., and LeClerc, J. E. (1986) Sequence dependence for bypass of thymine glycols in DNA by DNA polymerase I, *Nucleic Acids Res. 14*, 1045−1061.
39. Clark, J. M., and Beardsley, G. P. (1986) Thymine glycol lesions terminate chain elongation by DNA polymerase I in vitro, *Nucleic Acids Res. 14*, 737−749.
40. Clark, J. M., and Beardsley, G. P. (1987) Functional effects of cis-thymine glycol lesions on DNA synthesis in vitro, *Biochemistry 26*, 5398−5403.
41. Efrati, E., Tocco, G., Eritja, R., Wilson, S. H., and Goodman, M. F. (1997) Abasic translesion synthesis by DNA polymerase beta violates the "A-rule". Novel types of nucleotide incorporation by human DNA polymerase beta at an abasic lesion in different sequence contexts, *J. Biol. Chem. 272*, 2559−2569.
42. Showalter, A. K., Lamarche, B. J., Bakhtina, M., Su, M. I., Tang, K. H., and Tsai, M.-D. (2006) Mechanistic comparison of high-fidelity and error-prone DNA polymerases and ligases involved in DNA repair, *Chem. Rev. 106*, 340−360.
43. Pinz, K. G., Shibutani, S., and Bogenhagen, D. F. (1995) Action of mitochondrial DNA polymerase gamma at sites of base loss or oxidative damage, *J. Biol. Chem. 270*, 9202−9206.
44. Haracska, L., Yu, S. L., Johnson, R. E., Prakash, L., and Prakash, S. (2000) Efficient and accurate replication in the presence of 7,8-dihydro-8-oxoguanine by DNA polymerase eta, *Nat. Genet. 25*, 458−461.
45. Zang, H., Irimia, A., Choi, J. Y., Angel, K. C., Loukachevitch, L. V., Egli, M., and Guengerich, F. P. (2006) Efficient and high fidelity incorporation of dCTP opposite 7,8-dihydro-8-oxodeoxyguanosine by *Sulfolobus solfataricus* DNA polymerase Dpo4, *J. Biol. Chem. 281*, 2358−2372.
46. Johnson, R. E., Haracska, L., Prakash, S., and Prakash, L. (2001) Role of DNA polymerase zeta in the bypass of a (6-4) TT photoproduct, *Mol. Cell. Biol. 21*, 3558−3563.
47. Kouchakdjian, M., Bodepudi, V., Shibutani, S., Eisenberg, M., Johnson, F., Grollman, A. P., and Patel, D. J. (1991) NMR structural studies of the ionizing radiation adduct 7-hydro-8-oxodeoxyguanosine (8-oxo-7H-dG) opposite deoxyadenosine in a DNA duplex. 8-Oxo-7H-dG(syn)·dA(anti) alignment at lesion site, *Biochemistry 30*, 1403−1412.
48. Kamiya, H., Murata-Kamiya, N., Fujimuro, M., Kido, K., Inoue, H., Nishimura, S., Masutani, C., Hanaoka, F., and Ohtsuka, E. (1995) Comparison of incorporation and extension of nucleotides in vitro opposite 8-hydroxyguanine (7,8-dihydro-8-oxoguanine) in hot spots of the c-Ha-ras gene, *Jpn J. Cancer Res. 86*, 270−276.
49. Efrati, E., Tocco, G., Eritja, R., Wilson, S. H., and Goodman, M. F. (1999) "Action-at-a-distance" mutagenesis. 8-Oxo-7,8-dihydro-2′-deoxyguanosine causes base substitution errors at neighboring template sites when copied by DNA polymerase beta, *J. Biol. Chem. 274*, 15920−15926.
50. Cartwright, J. L., Safrany, S. T., Dixon, L. K., Darzynkiewicz, E., Stepinski, J., Burke, R., and McLennan, A. G. (2002) The

g5R (D250) gene of African swine fever virus encodes a Nudix hydrolase that preferentially degrades diphosphoinositol polyphosphates, *J. Virol. 76*, 1415−1421.
51. Garcia-Escudero, R., Garcia-Diaz, M., Salas, M. L., Blanco, L., and Salas, J. (2003) DNA polymerase X of African swine fever virus: insertion fidelity on gapped DNA substrates and AP lyase activity support a role in base excision repair of viral DNA, *J. Mol. Biol. 326*, 1403−1412.
52. Oliveros, M., Yanez, R. J., Salas, M. L., Salas, J., Vinuela, E., and Blanco, L. (1997) Characterization of an African swine fever virus 20-kDa DNA polymerase involved in DNA repair, *J. Biol. Chem. 272*, 30899−30910.
53. Einolf, H. J., Schnetz-Boutaud, N., and Guengerich, F. P. (1998) Steady-state and pre-steady-state kinetic analysis of 8-oxo-7,8-dihydroguanosine triphosphate incorporation and extension by replicative and repair DNA polymerases, *Biochemistry 37*, 13300−13312.
54. Kamath-Loeb, A. S., Hizi, A., Kasai, H., and Loeb, L. A. (1997) Incorporation of the guanosine triphosphate analogs 8-oxo-dGTP and 8-NH2-dGTP by reverse transcriptases and mammalian DNA polymerases, *J. Biol. Chem. 272*, 5892−5898.
55. Kung, H. C., and Bolton, P. H. (1997) Structure of a duplex DNA containing a thymine glycol residue in solution, *J. Biol. Chem. 272*, 9227−9236.
56. Miaskiewicz, K., Miller, J., Ornstein, R., and Osman, R. (1995) Molecular dynamics simulations of the effects of ring-saturated thymine lesions on DNA structure, *Biopolymers 35*, 113−124.
57. Furlong, E. A., Jorgensen, T. J., and Henner, W. D. (1986) Production of dihydrothymidine stereoisomers in DNA by gamma-irradiation, *Biochemistry 25*, 4344−4349.
58. Dizdaroglu, M. (1992) Oxidative damage to DNA in mammalian chromatin, *Mutat. Res. 275*, 331−342.
59. Martins, A., Ribeiro, G., Marques, M. I., and Costa, J. V. (1994) Genetic identification and nucleotide sequence of the DNA polymerase gene of African swine fever virus, *Nucleic Acids Res. 22*, 208−213.
60. Rodriguez, J. M., Yanez, R. J., Rodriguez, J. F., Vinuela, E., and Salas, M. L. (1993) The DNA polymerase-encoding gene of African swine fever virus: sequence and transcriptional analysis, *Gene 136*, 103−110.
61. Marques, M. I., and Costa, J. V. (1992) African swine fever virus-induced DNA polymerase is resistant to aphidicolin, *Virology 191*, 498−501.
62. Duarte, V., Muller, J. G., and Burrows, C. J. (1999) Insertion of dGMP and dAMP during in vitro DNA synthesis opposite an oxidized form of 7,8-dihydro-8-oxoguanine, *Nucleic Acids Res. 27*, 496−502.
63. Freisinger, E., Grollman, A. P., Miller, H., and Kisker, C. (2004) Lesion (in)tolerance reveals insights into DNA replication fidelity, *EMBO J. 23*, 1494−1505.
64. Miller, H., Prasad, R., Wilson, S. H., Johnson, F., and Grollman, A. P. (2000) 8-oxodGTP incorporation by DNA polymerase beta is modified by active-site residue Asn279, *Biochemistry 39*, 1029−1033.
65. Ishchenko, A. A., Yang, X., Ramotar, D., and Saparbaev, M. (2005) The 3′→5′ exonuclease of Apn1 provides an alternative pathway to repair 7,8-dihydro-8-oxodeoxyguanosine in *Saccharomyces cerevisiae*, *Mol. Cell. Biol. 25*, 6380−6390.
66. Tissier, A., McDonald, J. P., Frank, E. G., and Woodgate, R. (2000) poliota, a remarkably error-prone human DNA polymerase, *Genes Dev. 14*, 1642−1650.
67. Perrino, F. W., Harvey, S., Blans, P., Gelhaus, S., Lacourse, W. R., and Fishbein, J. C. (2005) Polymerization past the N2-isopropylguanine and the N6-isopropyladenine DNA lesions with the translesion synthesis DNA polymerases eta and iota and the replicative DNA polymerase alpha, *Chem. Res. Toxicol. 18*, 1451−1461.
68. Tissier, A., Frank, E. G., McDonald, J. P., Iwai, S., Hanaoka, F., and Woodgate, R. (2000) Misinsertion and bypass of thymine-thymine dimers by human DNA polymerase iota, *EMBO J. 19*, 5259−5266.
69. Zhang, Y., Yuan, F., Xin, H., Wu, X., Rajpal, D. K., Yang, D., and Wang, Z. (2000) Human DNA polymerase kappa synthesizes DNA with extraordinarily low fidelity, *Nucleic Acids Res. 28*, 4147−4156.
70. Ohashi, E., Ogi, T., Kusumoto, R., Iwai, S., Masutani, C., Hanaoka, F., and Ohmori, H. (2000) Error-prone bypass of certain DNA lesions by the human DNA polymerase kappa, *Genes Dev. 14*, 1589−1594.
71. Jarosz, D. F., Godoy, V. G., Delaney, J. C., Essigmann, J. M., and Walker, G. C. (2006) A single amino acid governs enhanced activity of DinB DNA polymerases on damaged templates, *Nature 439*, 225−228.
72. Suzuki, N., Ohashi, E., Hayashi, K., Ohmori, H., Grollman, A. P., and Shibutani, S. (2001) Translesional synthesis past acetylaminofluorene-derived DNA adducts catalyzed by human DNA polymerase kappa and *Escherichia coli* DNA polymerase IV, *Biochemistry 40*, 15176−15183.
73. Suzuki, N., Yasui, M., Geacintov, N. E., Shafirovich, V., and Shibutani, S. (2005) Miscoding events during DNA synthesis past the nitration-damaged base 8-nitroguanine, *Biochemistry 44*, 9238−9245.
74. Zhang, Y., Wu, X., Guo, D., Rechkoblit, O., Geacintov, N. E., and Wang, Z. (2002) Two-step error-prone bypass of the (+)- and (−)-trans-anti-BPDE-N2-dG adducts by human DNA polymerases eta and kappa, *Mutat. Res. 510*, 23−35.
75. Wolfle, W. T., Johnson, R. E., Minko, I. G., Lloyd, R. S., Prakash, S., and Prakash, L. (2006) Replication past a trans-4-hydroxynonenal minor-groove adduct by the sequential action of human DNA polymerases iota and kappa, *Mol. Cell. Biol. 26*, 381−386.
76. Washington, M. T., Johnson, R. E., Prakash, L., and Prakash, S. (2002) Human DINB1-encoded DNA polymerase kappa is a promiscuous extender of mispaired primer termini, *Proc. Natl. Acad. Sci. U.S.A. 99*, 1910−1914.
77. Johnson, R. E., Washington, M. T., Prakash, S., and Prakash, L. (2000) Fidelity of human DNA polymerase eta, *J. Biol. Chem. 275*, 7447−7450.
78. McCulloch, S. D., Kokoska, R. J., Masutani, C., Iwai, S., Hanaoka, F., and Kunkel, T. A. (2004) Preferential cis-syn thymine dimer bypass by DNA polymerase eta occurs with biased fidelity, *Nature 428*, 97−100.
79. Yao, J., Dixon, K., and Carty, M. P. (2001) A single (6-4) photoproduct inhibits plasmid DNA replication in xeroderma pigmentosum variant cell extracts, *Environ. Mol. Mutagen. 38*, 19−29.
80. Albertella, M. R., Green, C. M., Lehmann, A. R., and O'Connor, M. J. (2005) A role for polymerase eta in the cellular tolerance to cisplatin-induced damage, *Cancer Res. 65*, 9799−9806.
81. Kokoska, R. J., McCulloch, S. D., and Kunkel, T. A. (2003) The efficiency and specificity of apurinic/apyrimidinic site bypass by human DNA polymerase eta and *Sulfolobus solfataricus* Dpo4, *J. Biol. Chem. 278*, 50537−50545.
82. Choi, J. Y., Zang, H., Angel, K. C., Kozekov, I. D., Goodenough, A. K., Rizzo, C. J., and Guengerich, F. P. (2006) Translesion synthesis across 1,n(2)-ethenoguanine by human DNA polymerases, *Chem. Res. Toxicol. 19*, 879−886.
83. Chiapperino, D., Cai, M., Sayer, J. M., Yagi, H., Kroth, H., Masutani, C., Hanaoka, F., Jerina, D. M., and Cheh, A. M. (2005) Error-prone translesion synthesis by human DNA polymerase eta on DNA-containing deoxyadenosine adducts of 7,8-dihydroxy-9,10-epoxy-7,8,9,10-tetrahydrobenzo[a]pyrene, *J. Biol. Chem. 280*, 39684−39692.
84. Perrino, F. W., Blans, P., Harvey, S., Gelhaus, S. L., McGrath, C., Akman, S. A., Jenkins, G. S., LaCourse, W. R., and Fishbein, J. C. (2003) The N2-ethylguanine and the O6-ethyl- and O6-methylguanine lesions in DNA: contrasting responses from the "bypass" DNA polymerase eta and the replicative DNA polymerase alpha, *Chem. Res. Toxicol. 16*, 1616−1623.
85. Avkin, S., and Livneh, Z. (2002) Efficiency, specificity and DNA polymerase-dependence of translesion replication across the oxidative DNA lesion 8-oxoguanine in human cells, *Mutat. Res. 510*, 81−90.
86. Tang, M., Pham, P., Shen, X., Taylor, J. S., O'Donnell, M., Woodgate, R., and Goodman, M. F. (2000) Roles of *E. coli* DNA polymerases IV and V in lesion-targeted and untargeted SOS mutagenesis, *Nature 404*, 1014−1018.
87. Tang, M., Shen, X., Frank, E. G., O'Donnell, M., Woodgate, R., and Goodman, M. F. (1999) UmuD′(2)C is an error-prone DNA polymerase, *Escherichia coli* pol V, *Proc. Natl. Acad. Sci. U.S.A. 96*, 8919−8924.
88. Shen, X., Sayer, J. M., Kroth, H., Ponten, I., O'Donnell, M., Woodgate, R., Jerina, D. M., and Goodman, M. F. (2002) Efficiency and accuracy of SOS-induced DNA polymerases replicating benzo[a]pyrene-7,8-diol 9,10-epoxide A and G adducts, *J. Biol. Chem. 277*, 5265−5274.
89. Fuchs, R. P., Koffel-Schwartz, N., Pelet, S., Janel-Bintz, R., Napolitano, R., Becherel, O. J., Broschard, T. H., Burnouf, D. Y., and Wagner, J. (2001) DNA polymerases II and V mediate

respectively mutagenic (-2 frameshift) and error-free bypass of a single N-2-acetylaminofluorene adduct, *Biochem. Soc. Trans. 29*, 191−195.
90. Fiala, K. A., and Suo, Z. (2004) Pre-steady-state kinetic studies of the fidelity of *Sulfolobus solfataricus* P2 DNA polymerase IV, *Biochemistry 43*, 2106−2115.
91. Boudsocq, F., Iwai, S., Hanaoka, F., and Woodgate, R. (2001) *Sulfolobus solfataricus* P2 DNA polymerase IV (Dpo4): an archaeal DinB-like DNA polymerase with lesion-bypass properties akin to eukaryotic poleta, *Nucleic Acids Res. 29*, 4607−4616.
92. Perlow-Poehnelt, R. A., Likhterov, I., Scicchitano, D. A., Geacintov, N. E., and Broyde, S. (2004) The spacious active site of a Y-family DNA polymerase facilitates promiscuous nucleotide incorporation opposite a bulky carcinogen-DNA adduct: elucidating the structure-function relationship through experimental and computational approaches, *J. Biol. Chem. 279*, 36951−36961.
93. Zang, H., Goodenough, A. K., Choi, J. Y., Irimia, A., Loukachevitch, L. V., Kozekov, I. D., Angel, K. C., Rizzo, C. J., Egli, M., and Guengerich, F. P. (2005) DNA adduct bypass polymerization by *Sulfolobus solfataricus* DNA polymerase Dpo4: analysis and crystal structures of multiple base pair substitution and frameshift products with the adduct 1,N2-ethenoguanine, *J. Biol. Chem. 280*, 29750−29764.
94. Kobayashi, S., Valentine, M. R., Pham, P., O'Donnell, M., and Goodman, M. F. (2002) Fidelity of *Escherichia coli* DNA polymerase IV. Preferential generation of small deletion mutations by dNTP-stabilized misalignment, *J. Biol. Chem. 277*, 34198−34207.
95. Wagner, J., Gruz, P., Kim, S. R., Yamada, M., Matsui, K., Fuchs, R. P., and Nohmi, T. (1999) The dinB gene encodes a novel *E. coli* DNA polymerase, DNA pol IV, involved in mutagenesis, *Mol. Cell 4*, 281−286.

BI061501L